Supporting Information

Cold plasma activated Ni^0/Ni^{2+} interface catalysts for efficient electrocatalytic methane oxidation to low-carbon alcohols

Qiang Zhang[a,b*], Wei Li[a], Junyi Peng[a], Lian Xue[c], Ge He[d*]

a School of Chemistry & Chemical Engineering, Chongqing University of Technology, Chongqing 400054, P. R. China.

b National Engineering Laboratory for Methanol to Olefins, Dalian National Laboratory for Clean Energy, iChEM (Collaborative Innovation Center of Chemistry for Energy Materials), Dalian Institute of Chemical Physics, Chinese Academy of Sciences, Dalian 116023, P. R. China.

c Analytical and Testing Center, Chongqing University, Chongqing 404054, P. R. China.

d School of Chemical Engineering, Sichuan University, Chengdu 610065, P. R. China.

**Corresponding authors: Research School of Chemistry, Australian National University, ACT 2601, Australia.*

E-mail addresses: zqiang@cqut.edu.cn (Qiang Zhang); hege@scu.edu.cn (Junqiang Xu);

Mailing address for correspondence:

Qiang Zhang (A/Prof.)

School of Chemistry & Chemical Engineering, Chongqing University of Technology, Chongqing 400054, P. R. China.

E-mail: zqiang@cqut.edu.cn

In all measurements, we used SCE as the reference electrode. For comparison with the literature, all the potentials in this paper were converted to the RHE reference [S1]:

$$E\ (\text{vs. RHE}) = E\ (\text{vs. SCE}) + 0.24\ \text{V} + 0.059 * \text{pH}$$

CH_4OR was conducted in CH_4-saturated 0.1 M NaOH solution (pH=13 at room 25°Ctemperature and atmospheric pressure).

Faradaic efficiency (FE) of gaseous products at each applied potential was calculated based on the equation [S2]:

$$FE = \frac{\mathrm{z} \cdot \mathrm{P} \cdot \mathrm{F} \cdot \mathrm{V} \cdot v_i}{\mathrm{R} \cdot \mathrm{T} \cdot J}$$

Partial current density for C2 products normalized by the geometrical electrode area ($J_{\text{C2 products}}$, A cm^{-2}) was determined by calculating the total current density multiplied by FE of C2 products:

$$J_{\text{C2 products}} = FE_{C2\ products} \cdot J$$

C2 products mass activity was determined by C2 products partial current density divided by catalyst mass on the electrode:

$$\text{Mass activity} = \frac{J_{\text{C2 products}}}{\mathrm{m}}$$

C2 products production rate normalized by the geometrical electrode area (n, $mol \cdot cm^{-2} \cdot h^{-1}$) was calculated based on the formula:

$$n = \frac{\mathrm{P} \cdot \mathrm{V} \cdot v_i}{\mathrm{R} \cdot \mathrm{T}} \times 3600$$

Where z is the number of electrons transferred per mole of gas product (z is 4 for C2 products), F is Faraday constant (96500 $C \cdot mol^{-1}$), P is pressure (1.01 × 105 Pa), V is the gas volumetric flow rate (3.33×10^{-7} $m^3 \cdot s^{-1}$), v_i is the volume concentration of gas product determined by GC, T is the temperature (298.15 K), R is the gas constant (8.314

J $mol^{-1} \cdot K^{-1}$), J is the steady-state current at each applied potential (A), m is the catalyst mass on the electrode ($g \cdot cm^{-2}$).

To evaluate the effect of surface area, we measured the electrochemically active surface area (ECSA) for different catalysts electrodes from the electrochemical double-layer capacitance of the catalytic surface [1]. The electrochemical capacitance was determined by measuring the non-Faradaic capacitive current associated with double-layer charging from the scan-rate dependence of cyclic voltammograms (CVs). The double-layer charging current is equal to the product of the scan rate, v, and the electrochemical double-layer capacitance, CDL, as given by the equation:

$$i_c = vC_{DL}$$

Thus, a plot of i_c as a function of v yields a straight line with a slope equal to C_{DL}. The specific ECSA of the electrodes is calculated from the double layer capacitance according to the equation:

$$ECSA = C_{DL}/C_s$$

Where C_s is the specific capacitance of the sample or the capacitance of an atomically smooth planar surface of the material per unit area under identical electrolyte conditions. For our estimates of surface area, we use general specific capacitances of C_s = 0.020 mF based on typical reported values.

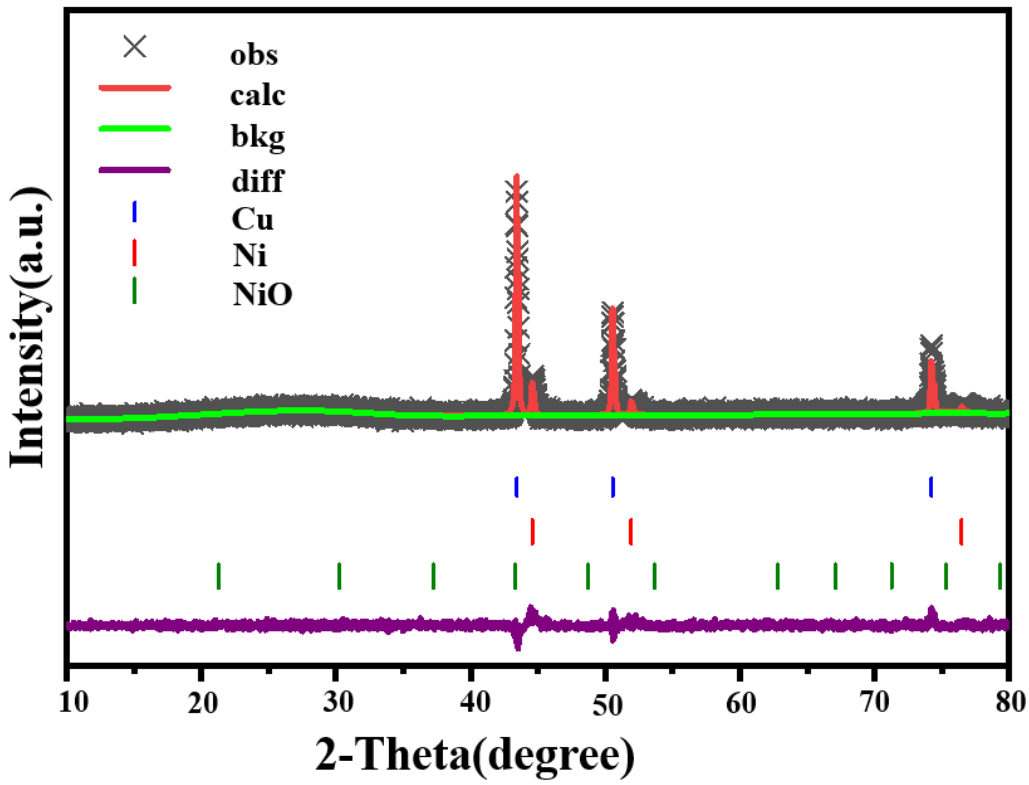

Fig. S1 Rietveld for Cu@Ni-NiO_x. (Rexp = 5.6%, Rwp = 14.0%, Rp = 11.5%, and Chi2 = 6.57)

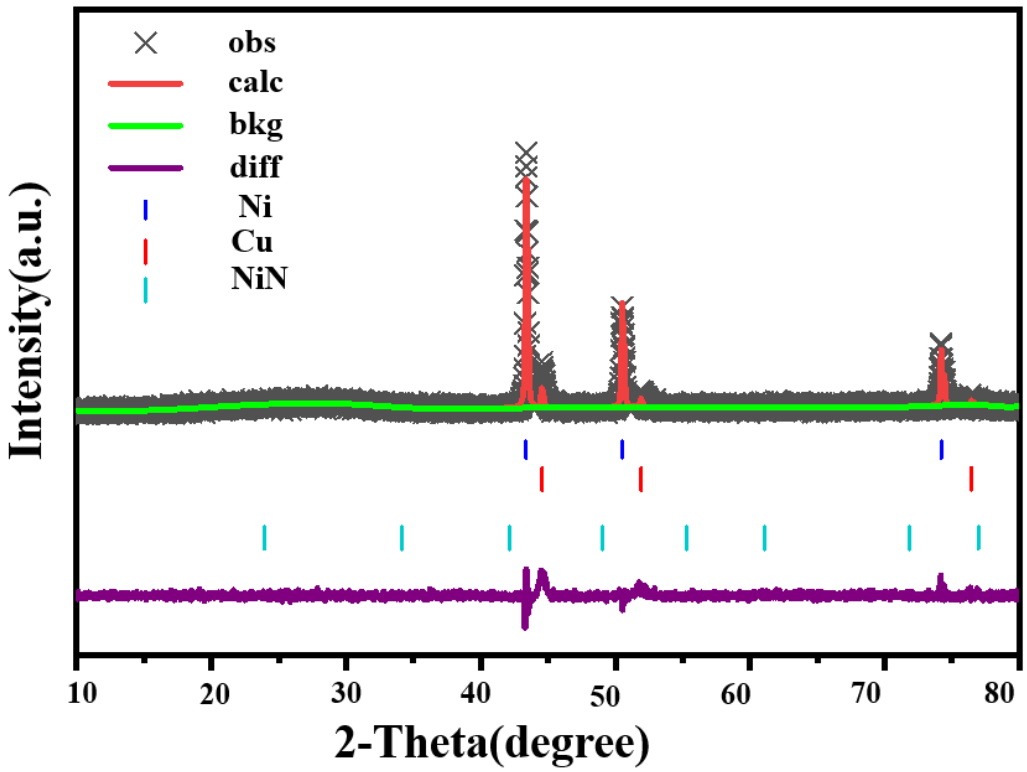

Fig. S2 Rietveld for Cu@Ni. (Rexp = 4.6%, Rwp = 13.7.0%, Rp = 12.5%, and Chi2 = 6.34)

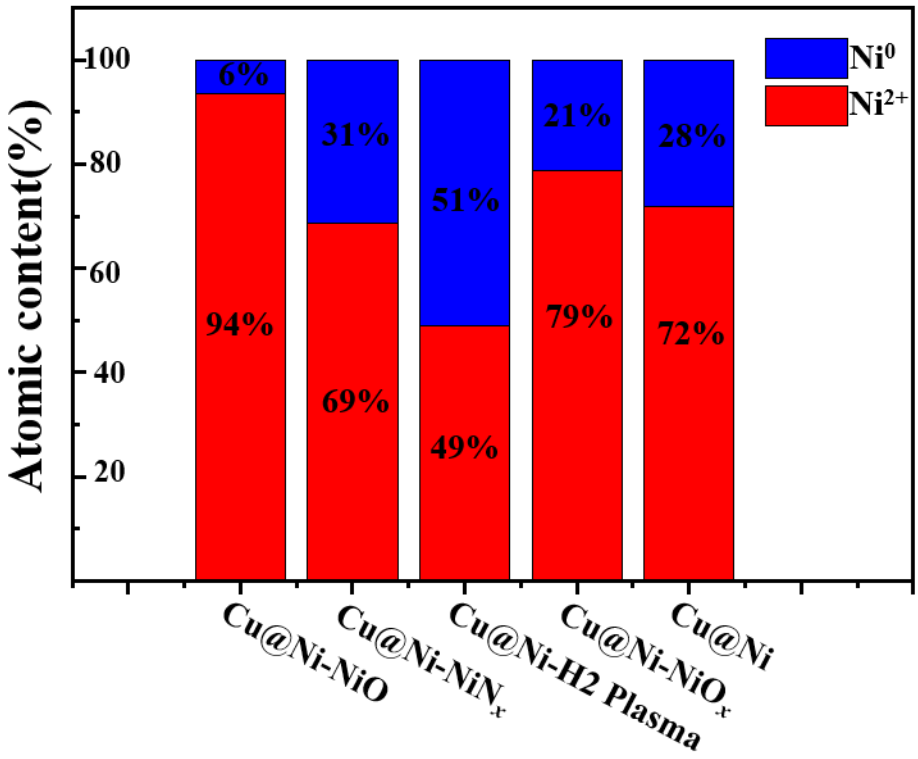

Fig. S3 The relative Ni^{2+}/Ni^{0} ratios of different catalysts.

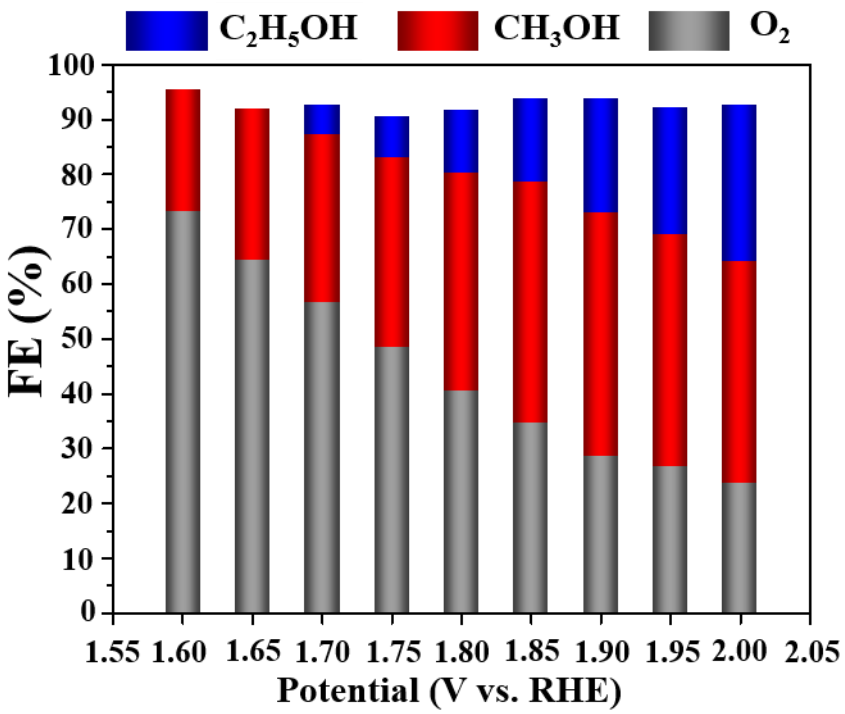

Fig. S4 FEs of the anodic products over Cu@Ni-NiO_x at various applied potentials.

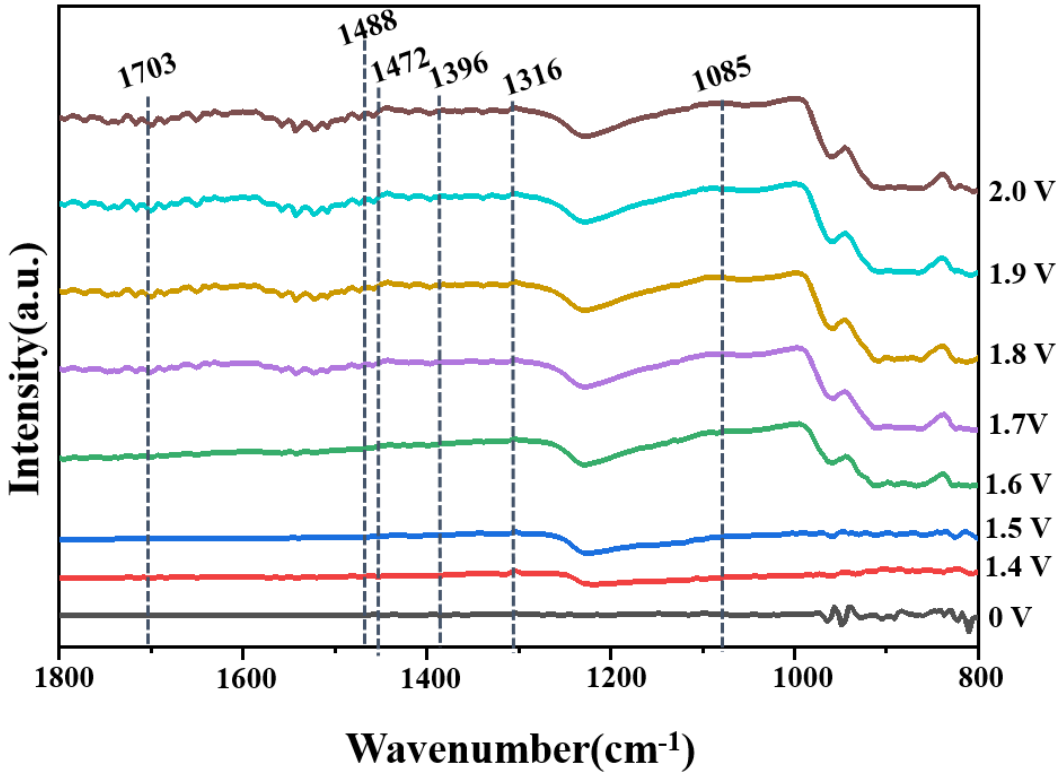

Fig. S5 In situ ATR-SEIRAS characterization for key intermediates against various time on Cu@Ni.

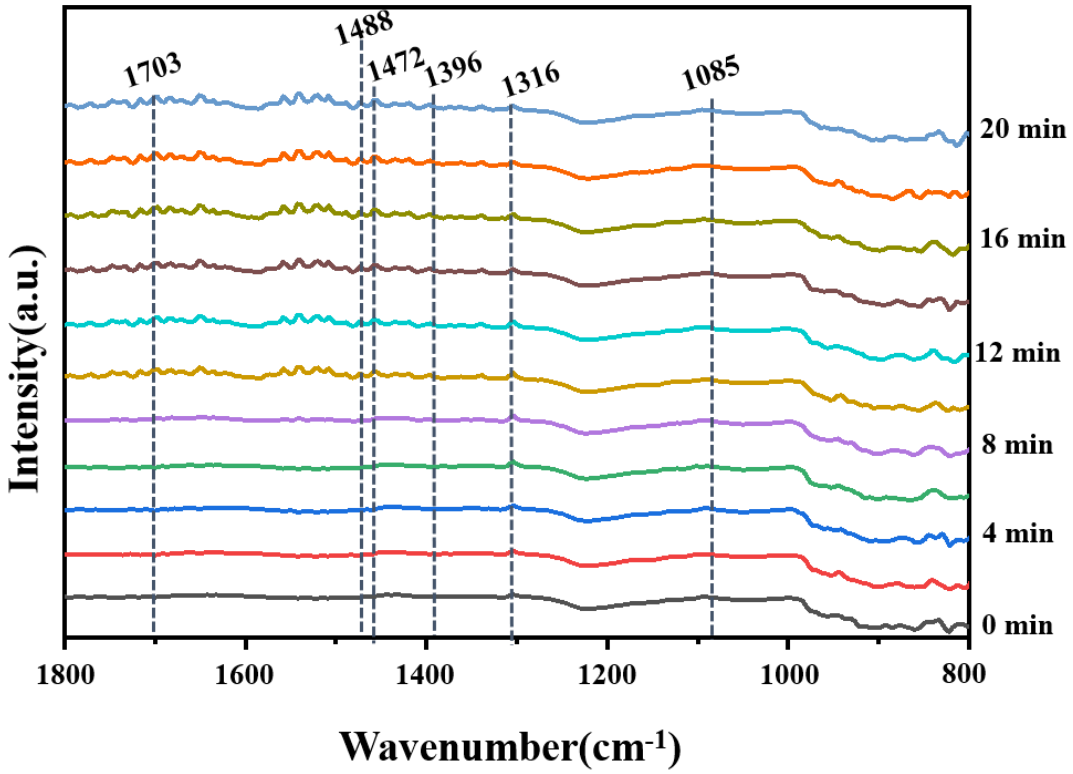

Fig. S6 In situ ATR-SEIRAS characterization for key intermediates against various potentials (0–2.0 V) on Cu@Ni.

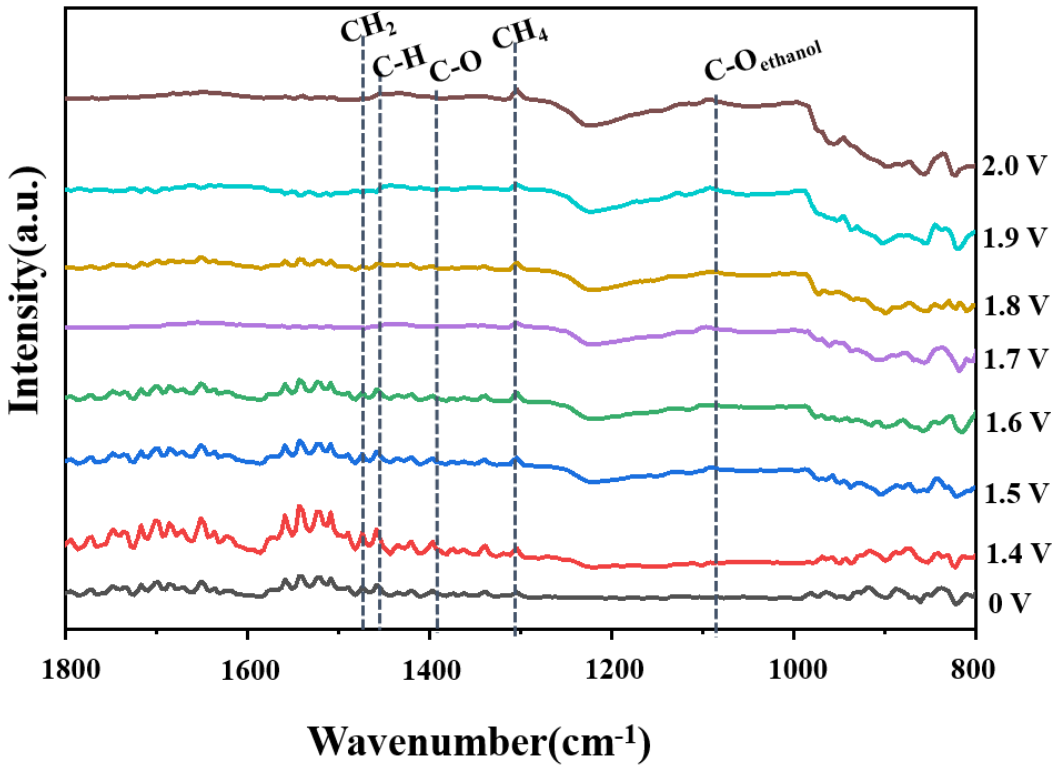

Fig. S7 In situ ATR-SEIRAS characterization for key intermediates against various time on Cu@Ni-NiO_x.

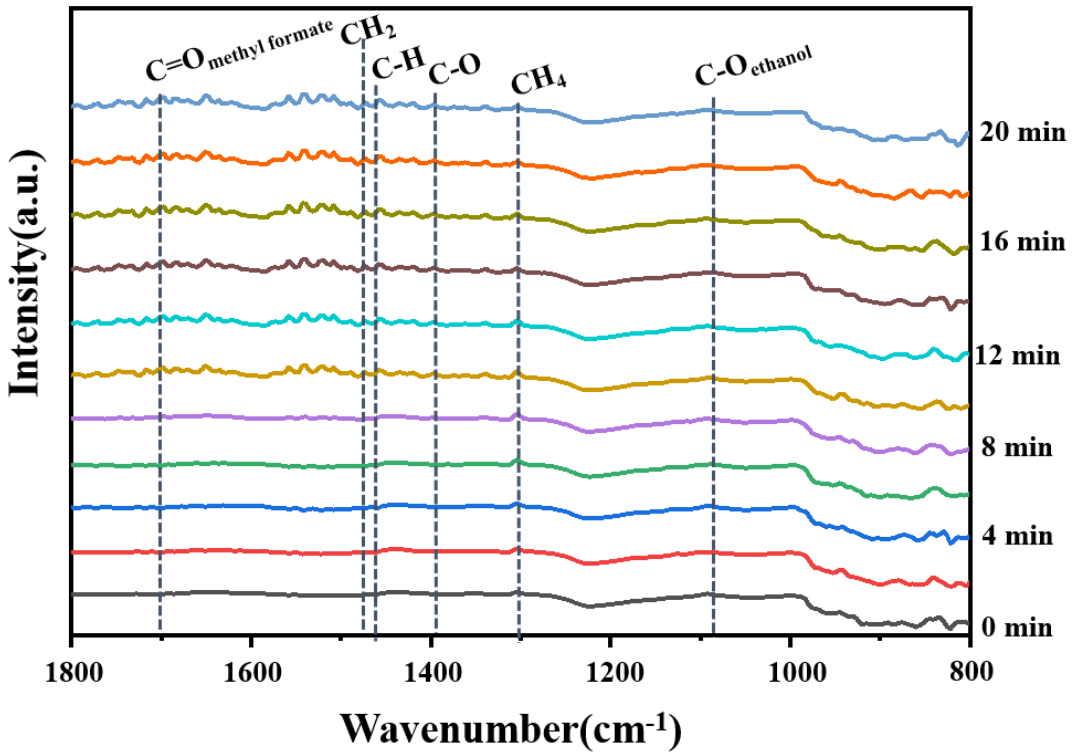

Fig. S8 In situ ATR-SEIRAS characterization for key intermediates against various potentials (0–2.0 V) on Cu@Ni-NiO_x.

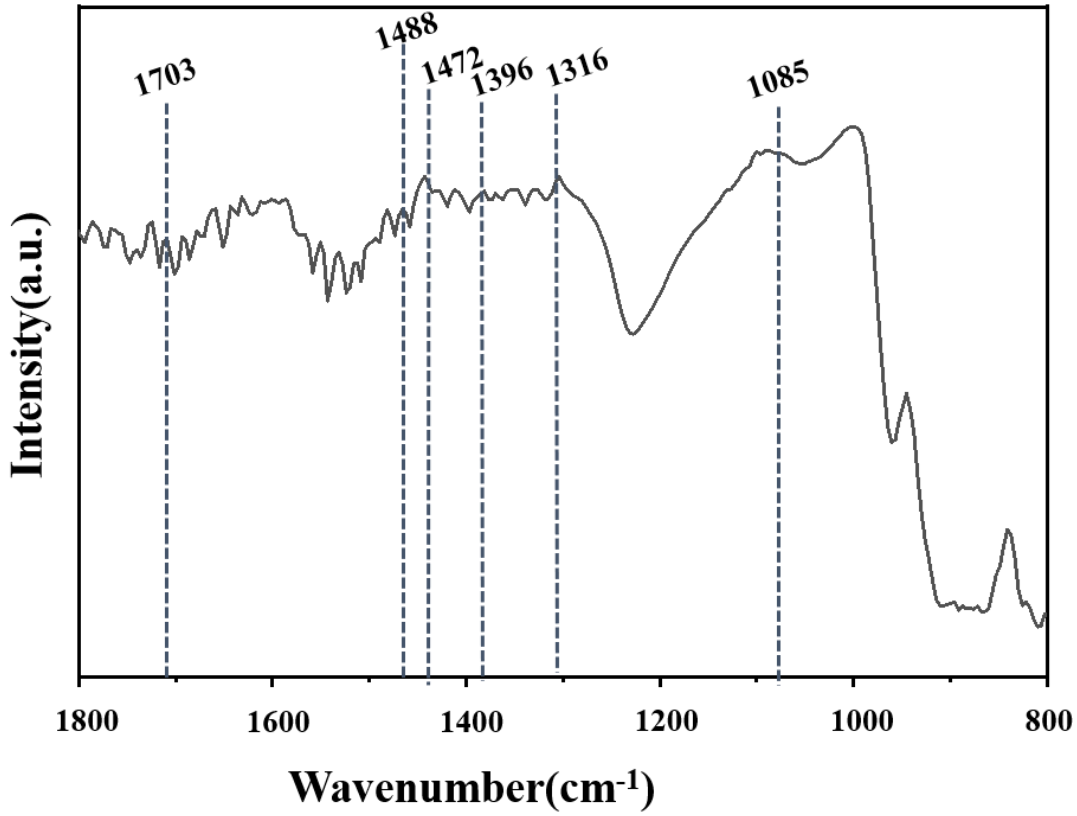

Fig. S9 In situ ATR-SEIRAS characterization for key intermediates on Cu@Ni-NiO_x at 1.9 V.

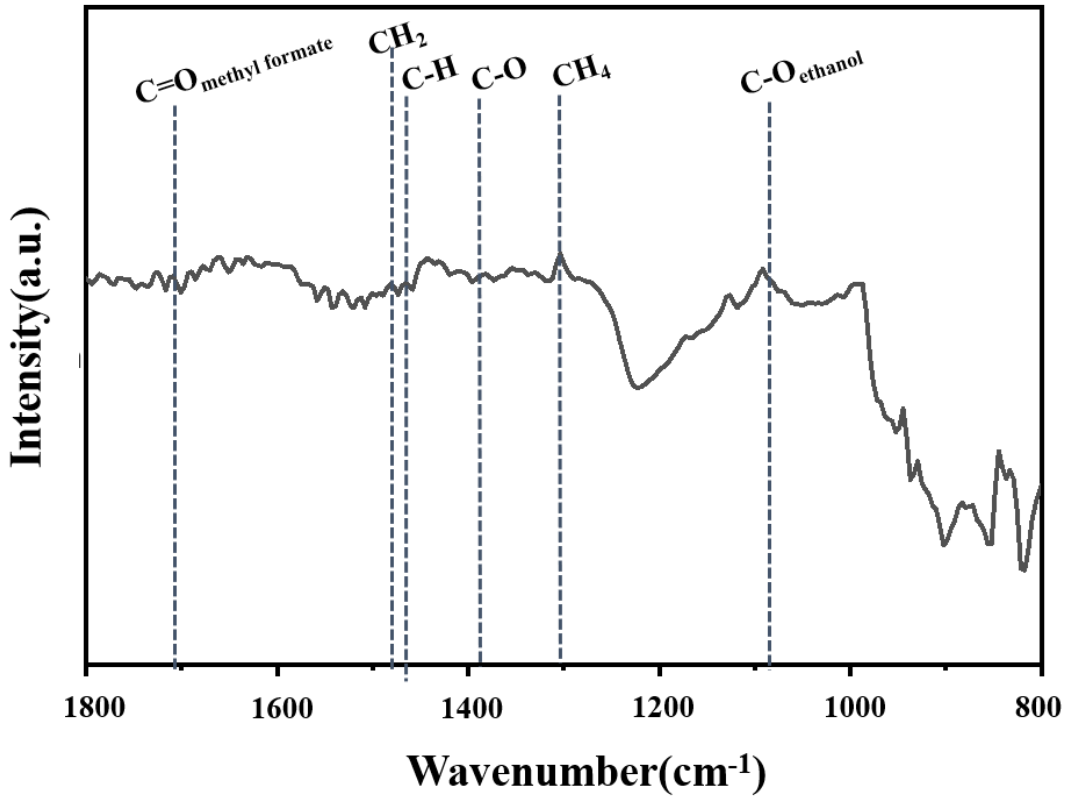

Fig. S10 In situ ATR-SEIRAS characterization for key intermediates on Cu@Ni-Ni at 1.9 V.

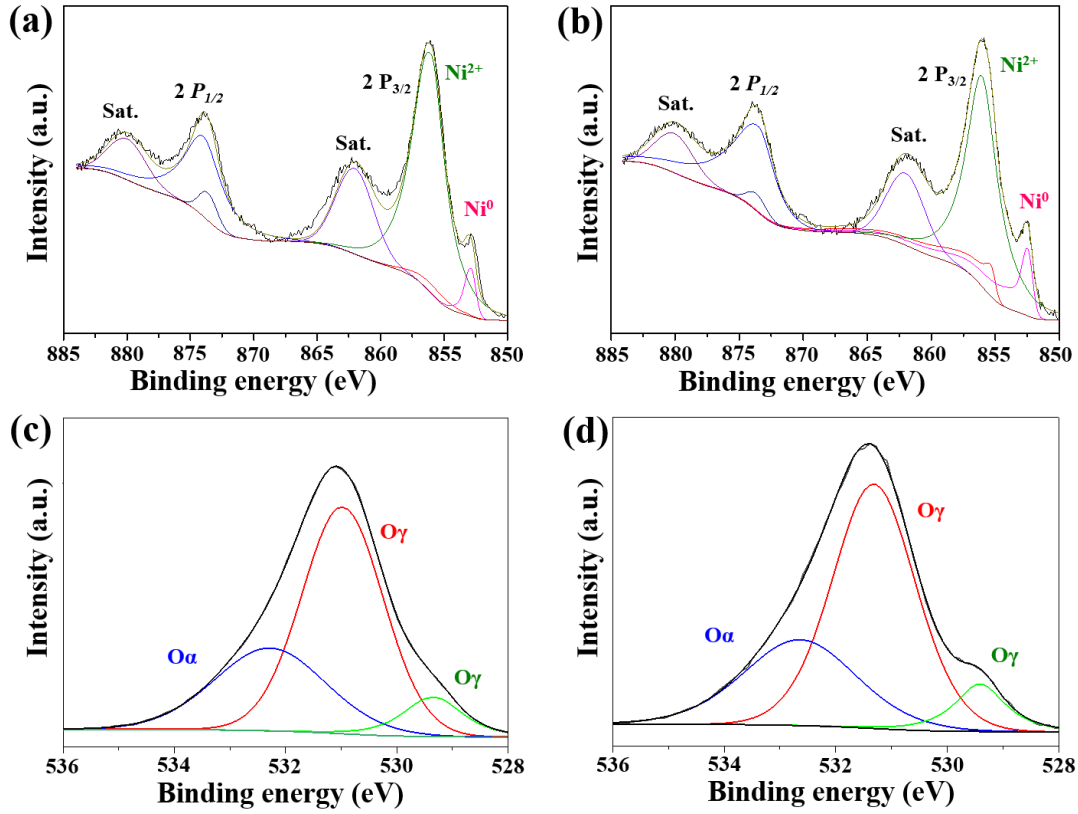

Fig. S11 High-resolution XPS spectra of Ni *2p* for Cu@Ni-NiO before (a) and after reaction(b). High-resolution XPS spectra of O *1s* for Cu@Ni-NiO before (c) and after reaction(d).

Table S1 Ni^0/Ni^{2+} ratio of Cu@Ni-NiO catalyst before and after applied potential (1.9 V *vs.* RHE, continuous electrolysis for 66 h).

Catalysts	Ni^0/Ni^{2+}
Cu@Ni-NiO	0.063
Cu@Ni-NiO-after	0.059

Table S2 Comparison with some reported performances of the catalysts for CH_4OR to alcohols.

Catalysts	Electrolyte	Potential (vs.RHE)	CH_3OH FE	C_2H_5OH FE	Total low-carbon alcohols	Stability (h)	Refs.
Cu@Ni-NiO	0.1 M NaOH	1.9 V	26.9%	59.8%	86.7%	66	This work
NiO/Ni	0.1M NaOH	1.4 V	-	89%	89%	25 h	[S3]
Ultrathin WO_3 nanosheets	0.1M Na_2SO_4	1.2 V	-	50.7%	50.7%	12 h	[S4]
Cu-Ti bimetallic oxides	1 M KCl	2.71 V	28%	-	28%	-	[S5]
Iron-nickel hydroxide nanosheets	0.1 M NaOH	1.46 V	~5%	87%	92%	2.5 h	[S6]
NiO/Ni hollow fiber	0.1M NaOH	1.44 V	-	85%	85%	3 h	[S7]
Cu_2O_3-TiO_2	0.1 M potassium phosphate buffer	2.15 V	~5%	-	5%	-	[S8]

References

[S1] M. Ferri, L. Delafontaine, S. Guo, T. Asset, P. Cristiani, S. Campisi and P. Atanassov, ACS Energy Letters., 2022, **7**, 2304-2310.

[S2] Q. Wang, M. Dai, H. Li, Y. R. Lu, T. S. Chan, C. Ma and M. Liu, Adv. Mater., 2023, 2300695.

[S3] Y. Song, Y. Zhao, G. Nan, W. Chen, Z. Guo, S. Li, Z. Tang, W. Wei and Y. Sun, Appl. Catal. B Environ., 2020, **270**, 118888.

[S4] J. Li, M. Luo, M. Wang, Y. Ma, G. Zheng, M. Wang, Y. Zhou, Y. Lu, C. Zhu and B. Chen, Appl. Mater. Today, 2023, **32**, 101855.

[S5] A. Prajapati, R. Sartape, N. C. Kani, J. A. Gauthier and M. R. Singh, ACS Catal., 2022, **12**, 14321-14329.

[S6] J. Li, L. Yao, D. Wu, J. King, S.S.C. Chuang, B. Liu and Z. Peng, Appl. Catal. B Environ., 2022, **316**, 121657.

[S7] Z. Guo, W. Chen, Y. Song, X. Dong, G. Li, W. Wei and Y. Sun, Chinese J. Catal., 2020, **41**, 1067-1072.

[S8] A. Prajapati, B. A. Collins, J. D. Goodpaster and M. R. Singh, P. Natl. Acad. Sci. USA., 2021, **118**, e2023233118.